UNIVERSIDAD DE DISEÑO, INNOVACIÓN Y TECNOLOGÍA

UDIT: UNIVERSIDAD DE DISEÑO, INNOVACIÓN Y TECNOLOGÍA

ÁGORA CREATIVA

Artículos científicos

INVESTIGACIÓN

13-4-2024

Optimization of an innovative hybrid approach ZnO-Doped PVP nanofibers for electrical devices applications

Javeria Shah

Aryan Dilawar Khan

Mahidur R. Sarker

Aiyeshah Alhodaib

Ammar Khan

See next page for additional authors

Follow this and additional works at: https://sciencevalue.udit.es/articulos_cientificos

Authors

Javeria Shah, Aryan Dilawar Khan, Mahidur R. Sarker, Aiyeshah Alhodaib, Ammar Khan, Mukhlisa Soliyeva, Vineet Tirth, Saima Naz Khan, Khizar Hayat, Amnah Mohammed, Moamen S. Refat, N.M.A. Hadia, Asad Ali, and Abid Zaman

Results in Physics 60 (2024) 107664

Contents lists available at ScienceDirect

Results in Physics

journal homepage: www.elsevier.com/locate/rinp

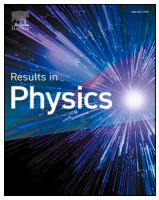

Optimization of an innovative hybrid approach ZnO-Doped PVP nanofibers for electrical devices applications

Javeria Shah [a,1], Aryan Dilawar Khan [b], Mahidur R. Sarker [c,d], Aiyeshah Alhodaib [e], Ammar Khan [a], Mukhlisa Soliyeva [f], Vineet Tirth [g,h], Saima Naz Khan [a], Khizar Hayat [a], Amnah Mohammed Alsuhaibani [i], Moamen S. Refat [j], N.M.A. Hadia [k], Asad Ali [l,1,*], Abid Zaman [m,*]

[a] Department of Physics, Abdul Wali Khan University Mardan 23200, Pakistan
[b] Department of Physics, Government College University of Lahore, Pakistan
[c] Institute of Visual Informatics, Universiti Kebangsaan Malaysia, Bangi 43600, Selangor, Malaysia
[d] Universidad de Diseño, Innovación y Tecnología, UDIT, Av. Alfonso XIII, 97, 28016 Madrid, Spain
[e] Department of Physics, College of Science, Qassim University, Buraydah 51452, Saudi Arabia
[f] Department of Physics and Teaching Methods, Tashkent State Pedagogical University, Tashkent, Uzbekistan
[g] Mechanical Engineering Department, College of Engineering, King Khalid University, Abha 61421, Asir, Kingdom of Saudi Arabia
[h] Centre for Engineering and Technology Innovations, King Khalid University, Abha 61421, Asir, Kingdom of Saudi Arabia
[i] Department of Physical Sports Sciences, College of Sports Sciences & Physical Activity, Princess Nourah bint Abdulrahman University, P.O. Box 84428, Riyadh 11671, Saudi Arabia
[j] Department of Chemistry, College of Science, Taif University, P.O. Box 11099, Taif 21944, Saudi Arabia
[k] Department of Physics, College of Science, Jouf University, Sakaka 2014, Al-Jouf, Saudi Arabia
[l] Department of Physics, Government Postgraduate College Nowshera, 24100 KP Pakistan
[m] Department of Physics, Riphah International University, Islamabad 44000, Pakistan

ARTICLE INFO

Keywords:
Zinc oxide NP's
Zinc oxide nanorods
Study-nanostructures
Electrospinning
Electrical and optical properties

ABSTRACT

The solid solution of pure ZnO nanoparticles and doped Polyvinylepyrrolidone (PVP) green hybrid nanomaterial's synthesized by using the electro spinning method. The synthetic polymer matrix nonwoven fibrous mats containing innovative properties are shown to shrink and encapsulated the zinc oxide materials to change the surface morphology when the concentration of PVP is increased from 1 % to 2 % dopants. The crystalline nature and morphological studies were examined by using x-ray diffraction and a scanning electron microscope. The average crystallite sizes of easily formed ZnO nanoparticles and nanorods that are 21 nm and 62 nm respectively. Moreover, the electrical and optical properties of the fibrous mesh were determined by using electrical impedance analyzer. The electrical conductivity values were measured in the pure ZnO nanoparticles in contrast to the doped ZnO/PVP. The tangent loss, dielectric constant, capacitance and relaxation time values are revealed in this study. All the characterization has been carried out at room temperature. The relaxation time for 1 %, and 2 % ZnO/PVP is (0.8 ns) and (0.79 ns) respectively which is suitable for the application of trigger using devices. The overall findings of this study implemented in a wide range of technologies i.e. photonics, electronics and super capacitor devices etc.

Introduction

Nanotechnology has emerged as a pivotal field in the 21st century, with nanoparticles (NP's) at the forefront of innovative technologies [1]. The nanoscale materials form the basis for a myriad of novel devices and patentable technologies. Understanding the fabrication and growth mechanisms of nanostructures materials are crucial for their wide spread application various scientific fields [2]. Materials within the nanoscale range of 1 to 100 nm, termed as nanomaterials, possess many applications in diverse sectors such as healthcare, medicine, food packaging, textiles, and cosmetics [3]. The synthesis of nanomaterials

* Corresponding authors.
E-mail addresses: kasadiiui@gmail.com (A. Ali), zaman.abid87@gmail.com (A. Zaman).
[1] These authors contributed equally to this work.

https://doi.org/10.1016/j.rinp.2024.107664
Received 19 January 2024; Received in revised form 7 April 2024; Accepted 10 April 2024
Available online 13 April 2024
2211-3797/© 2024 The Authors. Published by Elsevier B.V. This is an open access article under the CC BY license (http://creativecommons.org/licenses/by/4.0/).

can be achieved through either top-down or bottom-up approaches. A noteworthy success in the top-down approach is the synthesis of (1, 2 %) ZnO/PVP nanomaterials. [4] ZnO and PVP represent distinct nanomaterial structures, each possessing unique characteristics. Metal precursors play a vital role in the formation of Metal Oxide Nanoparticles (MONP's), contributing significantly to material sciences, chemical sciences, and physical sciences. ZnO/PVP NP's as a suitable candidate material among different size NP's due to its optimum optical, structural, microstructural and dielectric properties for multiple applications i.e. paint, absorption, rubber additives, gas sensors and super capacitors etc. [5,6]. The PVP blends have gained prominence in recent years due to their eco-sustainability, nontoxicity, biocompatibility, long-term stability, and cost-effectiveness arising from water solubility. PVP, being an amorphous polymer, exhibits high conductivity, transparency, hydrophobicity, and excellent film-forming properties [7,8]. The compatibility between ZnO and PVP matrices are attributed to interchain hydrogen bonding, making PVP a suitable host matrix for various dopant materials. This has prompted extensive research, resulting in the development of hybrid blend nanostructures that exhibit enhanced physical and chemical properties, expanding their potential applications. In the realm of PVP blends, various metal oxides such as $LiMnO_4$, MgO, TiO_2, SnO_2, SnO, Gd_2O_3, CuO, and ZnO etc, have been explored as dopants [9–15]. Notably, ZnO-doped 1 % PVP and 2 % PVP have demonstrated outstanding performance. This research sets the stage for a deeper exploration of the electrical and optical properties of ZnO/PVP compositions, providing a foundation for their potential applications in various industries [16]. PVP Nano fibers (NF's) exhibited spherical like structure with irregularly surface morphological shape ZnO nanoparticles (NP's). Conversely, 1 % PVP nanorods (NR's), as a result of doping, manifest as elongated rod-like structures characterized by a one-dimensional (1D) morphology. This diversification in structure imparts unique characteristics of the nanomaterial. ZnO NR's have longer structures and a different surface area profile than their nanoparticle equivalents. ZnO NR's and NP's are both often produced, each serving a particular purpose depending on its structural characteristics. Polymer materials are outstanding options for fiber manufacturing using semiconductor electrospinning processes. These methods improve the applicability of ZnO NR's and NP's for electrical applications while also making it easier to integrate them into polymeric matrices [17]. We start the synthesis and characterization of a correlated with concentration of ZnO-based polymeric NP's in the framework of our current investigation. We conduct a thoroughly investigation of the related structural, microstructural, optical, and dielectric properties of the samples by using the electro spinning technique. The aim of this study to clarify the complex nature of concentration-dependent changes while offering a deeper understanding of how these elements affected the general characteristics of NP's. Our study is designed to provide new important understandings into the possible uses of the polymeric based nanostructures materials. We have investigated the suitability of many characterizations of the samples particularly structure, microstructure, electrical, optical and dielectric properties. The finding of our research work has creating the opportunities for multiple applications.

Experimental procedure

Materials

Zinc nitrate Hexahydrate. ($Zn(NO_3)_2{\cdot}6H_2O$, 99.5 %), polyvinylpyrrolidone (PVP) $(C_6H_9NO)n$, and sodium hydroxide (NaOH, 99 %), were purchased from Sigma Aldrich chemicals Germany.

Preparation of ZnO/PVP

The solid solution of pure ZnO NP's and doped with various PVP composition was synthesized by using co-precipitation and electro spinning methods. This sophisticated procedure be revealed within the confines of the nanophysics laboratory at AWKUM, Pakistan, specifically within the Department of Physics. Initially, a homogeneous mixture was formulated by combining precise proportions of $Zn(NO_3)_2{\cdot}6H_2O$ (Sigma-Aldrich) prepared by co-precipitation methods. The solution experienced continuous stirring for 1 h, to obtained colloidal solution to appropriate quantity of NaOH solution was introduced to maintain a pH level within the range of 9–11. The mixture underwent uninterrupted stirring for 2 h until white precipitates emerged. Subsequently, the precipitated solution was filtered through filter paper and subjected to thorough washing with deionized water and ethanol, repeating the process three to five times. The resulting solution was subjected to another filtration step before undergoing drying at 80 °C for 2 h in an oven. The resulting sample was finely ground and subjected to annealing at 500 °C for 2 h in a box furnace under atmospheric air. Four distinct samples, specifically ZnO, were prepared following the aforementioned protocol. Moreover Polyvinylpyrrolidone (PVP) dopants, obtained from Sigma Aldrich Germany, were incorporated into the solution. Different concentrations of PVP (1 % and 2 %) were added to the prepared ZnO solution for each ratio. Subsequently, the ZnO/PVP solution used for electrospinning method was employed to produce the nano fibers, as depicted in Fig. 1.

Fabrication of Nano fibers (NF's)

Electro spinning technique as versatile and straight forward approach for producing NF's using electrostatic force, utilizing polymer solutions. A conventional electro spinning system typically comprises three main components: a spinneret (which supplies polymer sources), a high voltage power supply (for providing electric forces), and a collector (to gather nanofibers), as illustrated in Fig. 1. During the process, the polymer solution or melt forms a "Taylor cone" at the end of the spinneret as the spinning voltage gradually increases between the spinneret and the collector. Once the applied voltage beats a critical threshold, a polymer jet is ejected from the "Taylor cone" tip, solidifying into nanofibers upon reaching the collector. The electro spinning technique offers various attractive features, including simplicity, affordability, scalability for mass production, and wide-ranging applicability. Notably, electro spinning holds significant promise for recycling and reutilizing plastic waste, showcasing three primary advantages in this context. Moreover this critical phase, the resultant solution, now transformed into a dense, viscous fluid, was seamlessly transferred into a 10 ml syringe. Subsequently, this carefully prepared solution found its place within an electrospinning apparatus, where nanofibers were meticulously crafted. The culmination of this process involved allowing the freshly created nanofibers to undergo a thorough drying procedure before subjecting them to a rigorous evaluation. The generation of ZnO Nano rods (NR's)/PVP nanofibers mirrored the preceding procedure, it (2 %) as it too involved the insertion of the invented solution into a stainless-steel needle syringe depicted in Fig. 1. The electro spinning process resulted with precision, where an applied voltage of 12 kV and a controlled flow velocity of approximately 3 mm/hr were maintained. Crucially, the separation distance between the "Taylor cone" needle's tip and the collector was precisely set at 12 cm, ensuring optimal conditions for the formation of NF's. This synthesis method is undergoes to control the processing parameters to growth of ZnO NP's and NF's related phases within the medium of PVP.

Results and discussions

X-rays diffraction analysis

Fig. 2 shows the X-ray diffraction (XRD) pattern of ZnO, (1 %) PVP, PVP Nano fibers and (2 %) PVP. The XRD analysis revealed that the presence of dominant peaks all over the samples. The peaks that were identified from different diffractions that correspond to different crystallographic planes clearly indicate that ZnO has an intrinsic hexagonal

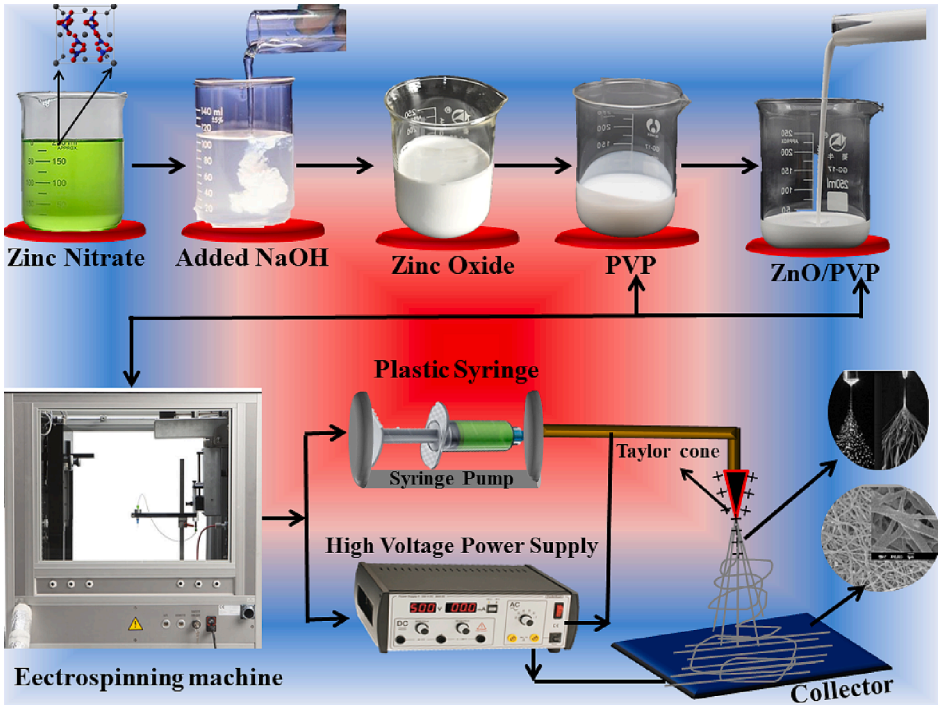

Fig. 1. Synthesis of PVP/ ZnO obtained for electro spinning method.

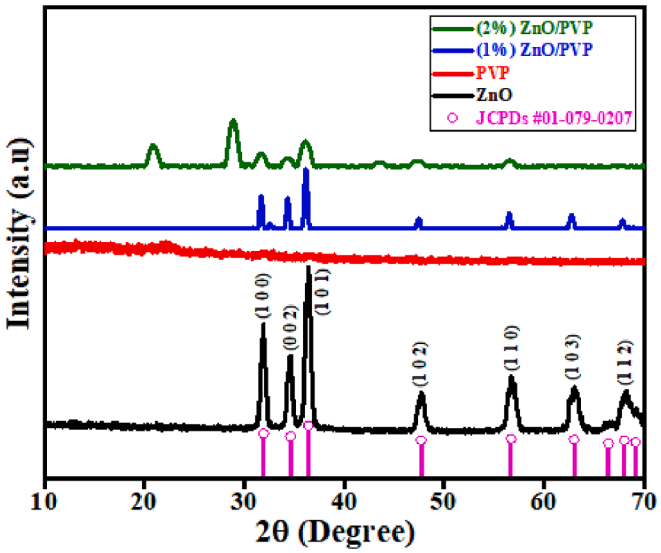

Fig. 2. XRD graph of pure ZnO, (1 %) PVP, PVP Nano fibers and (2 %) PVP.

structure. The clear identification of the hexagonal crystalline structure confirms that ZnO has been successfully integrated into the PVP copolymer matrix, demonstrating the accuracy and effectiveness of the synthesis technique used. An essential diagnostic technique, the XRD (JDX-3532, JEOL, Japan) investigation sheds light on the crystalline structure and conformance of the produced PVP copolymer-capped ZnO. The noticeable presence of characteristic peaks underscores the potential for targeted applications where the crystalline structure plays a key role in determining material properties and functionalities.

The structural properties of the prepared samples were examined by using X-ray powder diffraction technique. The data is displayed from 20° to 70°. Fig. 2 shows the sample's X-ray diffraction pattern. The measured diffraction peaks at 2θ = 31.699°, 34.382°, 36.182°, 47.495°, 56.87°, 62.760°, and 67.805° align with (1 0 0), (0 0 2), (1 0 1), (1 0 2), (1 1 0), (1 0 3), and (1 1 2) plans, that fits with JCPDS# 01–079-0207. The X-ray diffraction graph of the pure ZnO NP's showed wide peaks broadening, indicating the formation of Nano crystals [18]. The most prominent feature is that for all the samples with different plugging agents as well as for the pure sample the (1 0 1) peak is the strongest one. Additionally, the strong and narrow diffraction peaks make known the high purity, good crystallinity and size of the as prepared samples as far as the doping (1 %), and (2 %) PVP, the peak intensity decreases with broadness because the PVP is semi crystalline materials the crystal deformation show that loss crystallinity the final peak behavior is like semi crystalline. From XRD patterns of the filaments in an expansive top around 22° showed up, relating to PVP semi-crystalline in the Nano filaments [19]. The average crystallite size of ZnO NP's/PVP and ZnO NR's/PVP NF's is found to be 21.679 nm and 62 nm respectively by using Scherer-Debye formula despite the fact the crystallinity. When used to make materials, PVP polymer has low tensile strength, and low tensile stress lowers the FWHM and enhances crystallite size seen during creation [20].

Surface morphology

The intricated morphology of ZnO NP's was precisely investigated through the utilization of advanced imaging techniques, for utilizing a scanning electron microscope (SEM) (JSM-5910, JEOL Japan). The obtained images reveal a striking representation of the nanoscale features, separating a typical particle size within the range of approximately 50 nm as depicted in Fig. 3a. This dimension aligns with the prevalent standards for ZnO NP's, showcasing a meticulous control over the synthesis process [21]. Furthermore, the topography of the pure PVP unfolds as a network of finely spun nanofibers, as observed in the Fig. 3b. Notably, the introduction of a 1 % PVP dopant induces a distinct transformation, wherein nanorods emerge with a discernible clustering tendency, marked by considerable porosity. These unique Nano rods in Fig. 3c formation can be attributed to the Brownian effect of PVP molecules, orchestrating a performance that leads to stacking the Nano rods with a distinct structure [22]. The growth rates of PVP contribute significantly, resulting in the observed nanorods morphology with dimensions ranging between 50 nm and 70 nm, presents SEM images

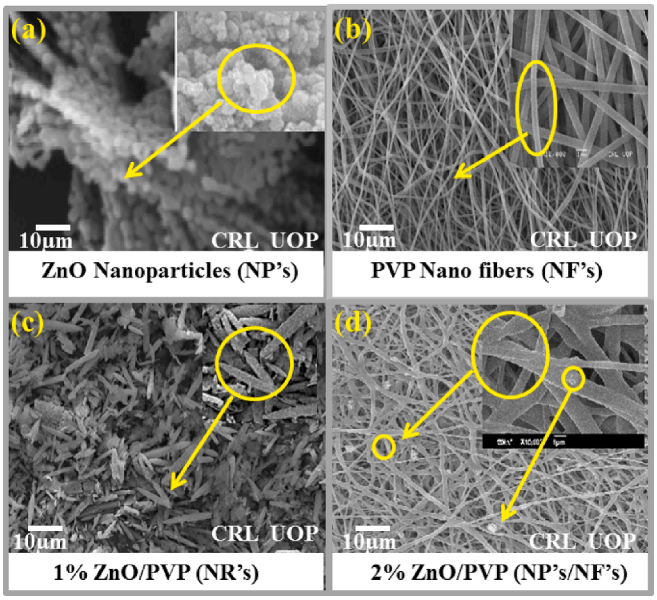

Fig. 3. Scanning electron microscopy images (SEM) of **(a)** ZnO NP's **(b)** PVP NF's **(c)** ZnO/PVP- NR's **(d)** ZnO/PVP- NF's.

capturing the morphological intricacies of ZnO doped with 2 % PVP. Remarkably, this configuration exhibits a compelling manifestation of completely formed nanofibers as illustrated in Fig. 3c interspersed with small nanoparticle clusters adhering to the fiber walls. These electro spun structures, originating from a pristine PVP matrix, showcase dimensions carefully measured at 310 nm, 520 nm, 549 nm, 860.8 nm, and 533.43 nm. The meticulous control over dimensions and morphology evident in these SEM images signifies a nuanced understanding of the doping process, laying the groundwork for tailored applications in diverse scientific and technological domains [23].

Electrical properties

AC conductance analysis

Our investigation employed an impedance analyzer (Agilent-E4991A) spanning frequencies from 10 Hz to 2 MHz to assess the conductance (G) of samples held at room temperature. The results, depicted in Fig. 4, reveal a distinctive trend in conductance values concerning variations with frequency. Fig. 4 illustrates a noticeable rise in conductance values with increasing frequency for all samples. This behavior is ascribed to the influence of the hopping conduction mechanism, which significantly shapes the electrical characteristics of the samples. Two distinct zones are present, according to the data collected by the impedance analyzer. The first region appears at lower frequencies, when the electric field is not strong enough to cause hopping conduction mechanisms. This region has two conflicting relaxation processes, the unsuccessful hop and the successful hop, and is intimately related to DC conductance. These findings provide important new information on the complicated interaction between conductance and frequency in our samples. The patterns that have been seen demonstrate how crucial the hopping conduction process is in shaping the electrical features, providing a deeper understanding of the underlying processes governing the material's dynamic response. The electrical conductivity of ZnO and PVP related samples are varies due to increasing doping concentration [24–27].

Moreover the increasing the ac conductivity at high frequency maybe due to many factors, like increase in temperature, higher frequencies, shifting of peaks towards Bragg's angles, different kind of polarization phenomena, variation in particle size, and relative densities etc. Which shows the variations in ac conductivity of pure ZnO NP's and (1 %) doped ZnO/PVP composition. In case of dielectrics, the mechanism of polarization can be described in terms of discontinuous hopping of charges [28,29]. As per jump relaxation model (JRM), the ac conductivity is correlated with the narrow unsuccessful hopping of electrons or ions [30,31]. Furthermore, the appearance of unsuccessful hop rises with frequency. And thus, the high frequency domain shows the localized or reorientation hopping processes. Therefore, the forward–backward jumping mechanism, that is "unsuccessful hops," leads the ac conductivity process [32].

Resistance analysis

The relationship between resistance and frequency that was gathered in the 10 Hz to 2 MHz range has been measured by using LCR meter (Chroma 11021/11021-L) as shown in the Fig. 5 observed various resistance values for various samples at the same frequency. The nano materials at room temperature was used to calculate the resistance values for the ZnO NP's, and doped PVP Nano fibers shows different behavior. A decrease in resistance occurs when certain electrons in semiconductive materials build up thermal energy and break through the

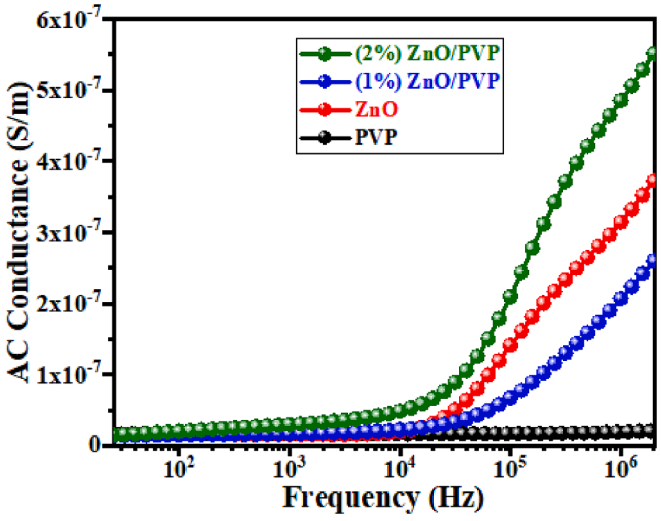

Fig. 4. Frequency versus AC Conductivity of PVP, ZnO, 1 % ZnO/PVP & 2 % ZnO/PVP compositions.

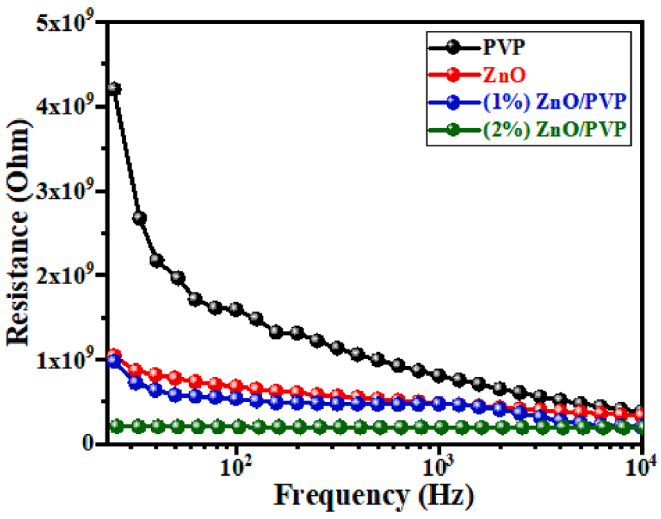

Fig. 5. Frequency versus Resistance of PVP, ZnO, 1 % ZnO/PVP & 2 % ZnO/PVP compositions.

barrier splitting the valance and conduction bands [33]. A little amount of energy is needed to initiate the conduction process. The resistance value of pure PVP is reported 4250 MΩ which is decreases to 250 MΩ with 2 % ZnO/PVP composition. Due to the low resistance values of ZnO/PVP Nano fibers, charges will flow smoothly throughout the samples which are helpful for making electrical devices [34,35].

Dielectric constant

The convoluted relationship between dielectric constant and frequency is brightly shown in the Fig. 6 and has been measured by using impedance analyzer (Agilent-E4991A, USA) spectroscopy. The dispersion behavior loosens a relationship, highlighting a distinctive inverse correlation between frequency and dielectric constant. In our investigation, ZnO NP's −doped Nano fibers with varying PVP concentrations (1 % and 2 %) were studied. Notably, the dielectric constants for these nanofibers are found to be 7.8 and 24, respectively. The overall values of dielectric constant for all samples decreases with increasing frequency (see Fig. 6). At lowest frequency highest value of dielectric constant (45) is recorded at 2 % ZnO/PVP which is suitable for the application of dielectric resonator antenna. The significant difference in dielectric constants positions the 2 % PVP NF's as insulators, surpassing their 1 % counterpart. This observation emphasizes the key role of dopant concentration in influencing dielectric properties. Furthermore, a comprehensive comparison of the effects of various dopant materials, particularly at concentrations of 1 % and 2 %, underscores the pronounced impact of increased dopant materials. The enhanced dielectric constant performance exhibited by the 2 % PVP Nano fibers signifies superior energy storage capacity compared to their 1 % counterparts. High ε_r dielectrics, such as 2 % ZnO/PVP, have a dielectric constant of about 45, which means that they can store more charge per unit area, this finding opens new avenues for optimizing energy storage applications by tailoring dopant concentrations in NF's materials. The presented results not only contribute to the fundamental understanding of dielectric behavior in NF's composites but also cover the way for designing advanced materials with enhanced dielectric properties for diverse technological applications [36,37].

Tangent loss

Fig. 7 shows the tangent loss of the composition of a) PVP, b) ZnO, c) 1 % ZnO/PVP & d) 2 % ZnO/PVP. The Nano crystals ZnO NP's-doped

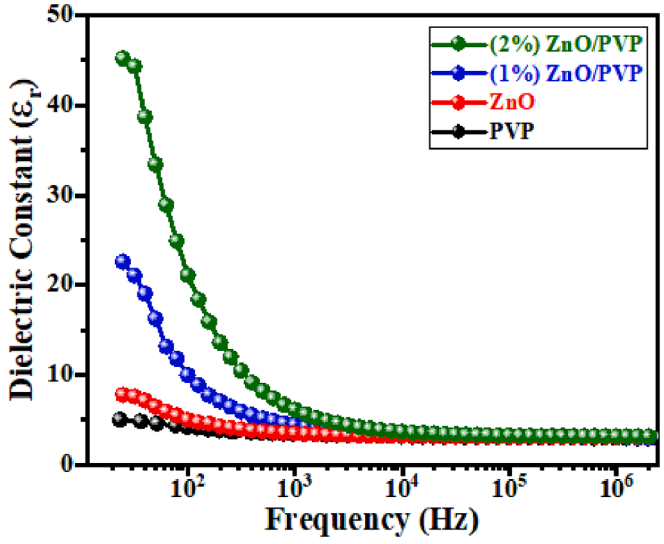

Fig. 6. Frequency versus Dielectric constant of PVP, ZnO, 1 % ZnO/PVP & 2 % ZnO/PVP compositions.

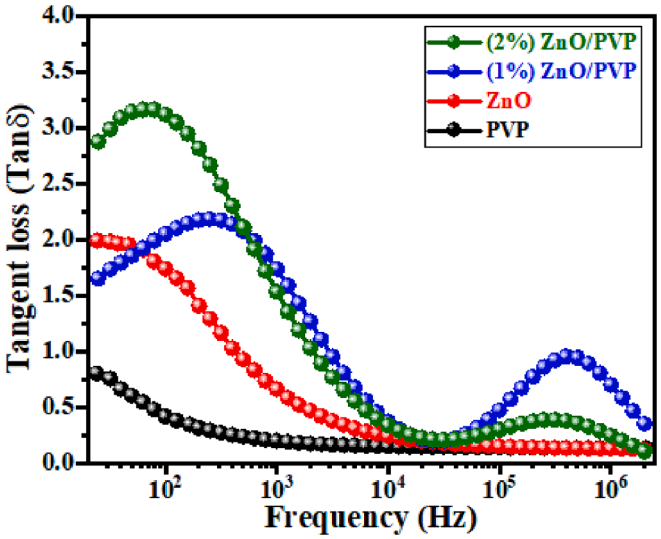

Fig. 7. Frequency versus Tan loss of PVP, ZnO, 1 % ZnO/PVP & 2 % ZnO/PVP compositions.

NF's with varying PVP concentrations (1 % and 2 %), the tangent loss is decreases with increasing PVP concentration and frequency as well. Moreover, the innovative materials NF's have a larger Tang loss value than (1 % PVP) NF's because to their higher dielectric constant value [33]. The dielectric loss, or energy lost as heat from the applied field into the sample, is proportional to the loss tangent (tan δ). Therefore, in dielectric schemes, the energy dissipation can be determined by loss tangent (tan δ), and it is expected that domain wall resonance supports it. Because domain wall motion is constrained and magnetization is forced to shift gyration at higher frequencies, this loss is often negligible [38]. The loss tangent variation with frequency for both pure and doped samples is shown in Fig. 7.

Dielectric Losses are particularly high around the relaxation or resonance frequencies of polarization mechanisms. The polarization delays the applied field, resulting in an interaction between the field and the Dielectric's polarization, leading to energy dissipation. These two peaks are in the Fig. 7 maybe due to the different kinds of polarizations mechanism and structural homogeneity [39]. Further the tangent loss peaks as a function of frequency is telling you something about the dissipation process that is producing the energy loss. It might correspond to a molecular Debye-type relaxation (dipole resonances or oscillating dipoles). In Debye type dielectric relaxation, such peaks are seen easily. The tan delta signal or graph is defined as the quotient of the loss modulus (mechanical) or dielectric loss and the storage modulus (mechanical) or permittivity (dielectric), respectively. When a loss peak is clearly evident, I prefer to use its spectrum over that of a tan delta. In mechanical measurements, the highest temperature peak in tan delta is taken to indicate the glass transition temperature (peak temperature). This sometimes carries over to dielectric measurements, but typically, dielectric measurements may indicate more tan delta peaks than one sees mechanically [40,41].

Impedance spectroscopy (IS)

Fig. 8 shows the variation of capacitance with frequency of a) PVP, b) ZnO, c) 1 % ZnO/PVP & d) 2 % ZnO/PVP compositions. The capacitance of the capacitor can also be influenced by the frequency of the signal that is present at its terminals and capacitive reactance as well. The reason for this phenomenon, known as dielectric dispersion, is because the dielectric's polarization lags behind the quickly varying signal. Capacitive reactance increases when the frequency is lower and decreases when the frequency is higher. The relationship between capacitive reactance and system frequency is inversely.

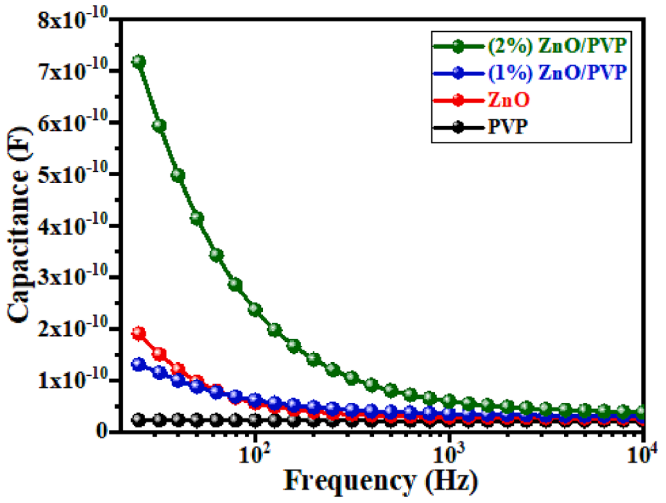

Fig. 8. Variation of Capacitance with Frequency of PVP, ZnO, 1 % ZnO/PVP & 2 % ZnO/PVP compositions.

The capacitance measurements show how the stabilizing agent and surfactant affect the metal oxide nanoparticles' specific capacitance [42]. Furthermore, the specific capacitance is greatly influenced by the precursors and synthesis techniques used to create NPs. Selecting the right precursors is crucial for increasing specific capacitance since synthesis-formed impurities can reduce conductivity [43]. The precursor used can also affect the size and shape of the particles, which can affect the working electrode's capacitance [44–46]. ZnO particles were produced by Alver et al. using several zinc precursors. The predecessors offer differences in ZnO particle morphologies and sizes, which affect the final material's specific capacitance [47]. Similar to this, the technique used is also important for calculating specific capacitance because the values rely on electron diffusion, which is directly related to the structure of the material being synthesized [48,49]. The ZnO/PVP exhibit a semicircle arc, which is proof that the addition of ZnO nanoparticles to the PVP changed the material's behavior from insulating to semi-conductive. The semicircle's diameter exhibits the resistance of the grain boundary the plot, it is obvious that dopant of 1 % – PVP NF's have a diameter semicircle. The diameter of the semicircle used to compute the grain boundary resistance (Rgb) for the samples is 8.1and 18 Ω [50]. Moreover, the electrical response of a substance is investigated using impedance spectroscopy. By using this method, it is possible to retrieve information about the material's conduction mechanism, relaxation events, and various contributions from the grain, grain border, and electrodes. Further, the instrument impedance analyzer was used to perform impedance spectroscopy (IS) the frequency used ranged from 10 Hz to 2 MHz. The data were shown in Fig. 9 by using a Nyquist diagram that includes both real and imaginary impedances [51]. In addition, figure's linear impedance response for PVP NF's is caused by the insulating properties of PVP. The data were shown in Fig. 10 by using a Nyquist graph, which includes imaginary impedance versus real impedance. As a result, the insulating qualities of PVP are the reason behind the linear impedance response for PVP NF's depicted in the picture [52,53].

Using the Arrhenius equation, we can compute the activation energy of various concentrations (1, 2 %) ZnO/PVP NF's numerically,

It is commonly known that the Arrhenius equation is

$$K = Ae^{-E_a/RT} \tag{1}$$

The activation energy, general gas constant, temperature, and the frequency factor are represented by the letters Ea, R, T, and A, respectively. Besides, identify an unidentified parameter k in order to obtain the activation energy.

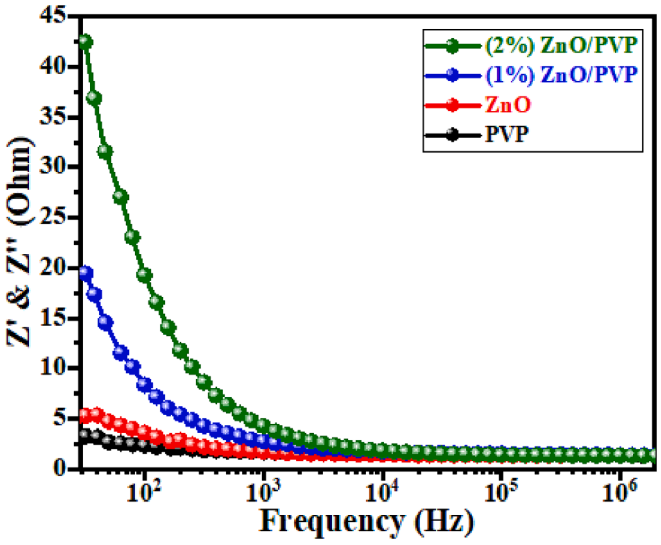

Fig. 9. Z', Z'' vs. Frequency plot of PVP, ZnO, 1 % ZnO/PVP & 2 % ZnO/PVP compositions.

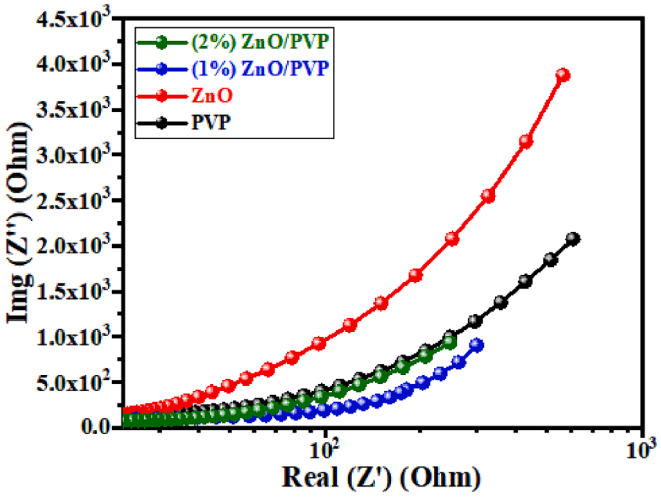

Fig. 10. Nyquist plot between Img (Z″) and real (Z') of PVP, ZnO, 1 % ZnO/PVP & 2 % ZnO/PVP compositions.

$$K = M/t$$

Here Molarity (M = 0.5148 mol/L)

Time (t = 24hrs or 1440 mins).

By putting these values in the above equation, we obtained the 'k' value is 0.00036 min^{-1}.

The activation energy possibly found by rearranging the Arrhenius equation, which is given by

$$E_a = -RT\ln(K/A) \tag{2}$$

Here

Room temperature (T = 300.15 K).

General gas constant (R = 8.1314 J/mol.k).

Frequency factor (A = 4 x 10^{13} s^{-1}).

By putting these values in equation (2) then we obtained the activation energy is 96.0 KJ/mole

Relaxation time is calculated by the given formula

$$\tau = RC \tag{3}$$

Capacitance (C) will be calculated by using the following formula

$$C = 1/2\pi fR \quad (4)$$

Here

Resistance (R = 9 Ω).

Frequency (f = 2 MHz).

Pi (π = 3.14).

By using these values 1 % Nano fibers in equation (4) we obtained the capacitance is 8.84 nF (Nano Farad).

The relaxation time (0.8 ns) for 1 % Nano fibers is obtained after putting the values of 'R' and 'C' in equation (3).

For 2 % Nano fibers composition, the capacitance values is 0.92 nanofarad while the relaxation time is 0.79 ns obtained by using the following parameters in equation (3) and (4).

Resistance (R = 86 Ω).

Frequency (f = 2 MHz).

Pi (π = 3.14).

The reported values of the relaxation time are suitable for trigger related application [50].

Conclusions

This study introduces a new approach for designing advanced materials by incorporating various concentrations of dopant (1 % and 2 %) of PVP with pure ZnO NP's.. Our investigations focus on revealing the different structural, microstructural, electrical and optical properties of these samples. Broad electrical assessments were conducted, including parameters such as electrical conductivity, capacitance, dielectric constant, and tangent loss. Notably, the AC conductance values of PVP NF's based on ZnO NR's and NP's were measured at 3.1×10^{-9} S/m and 4×10^{-9} S/m, respectively. Surprisingly, despite the larger size and narrower grain boundaries of NR's, NF's incorporating them exhibited lower resistance (250 MΩ) compared to those based on nanoparticles (4250 MΩ). Furthermore, 2 % dopant ZnO NR's/PVP NF's demonstrated superior dielectric constant (45) and capacitance values (0.92×10^{-9}F) compared to 1 % ZnO NP's/PVP NF's is (dielectric constant: 7.8, capacitance: 8.84×10^{-9}F). However, the study found higher tangent losses associated with 2 % PVP NF's, a factor deemed acceptable for the potential dielectric applications. Additionally, relaxation periods in NF's based on zinc oxide NR's (2 %) were found to be orders of magnitude slightly different than those in nanoparticle-based nanofibers (1 %). The main objective of this study is to investigate the impact of various dopant concentrations (1 % and 2 %) of PVP materials on pure ZnO NP's Explore the diverse electrical, structural, dielectric and optical properties exhibited by different dopant concentrations for innovative material applications. Conduct a comprehensive electrical evaluation, including parameters such as electrical conductivity, capacitance, real and imaginary impedance, dielectric constant, temporal relaxation, and tangent loss. Compare the electrical properties of AC conductance in PVP NF's based on zinc oxide Nano rods and nanoparticles. The overall findings of this study have been used for multiple applications.

CRediT authorship contribution statement

Javeria Shah: Writing – original draft, Conceptualization. **Aryan Dilawar Khan:** Writing – review & editing, Writing – original draft. **Mahidur R. Sarker:** Conceptualization, Formal Analysis. **Aiyeshah Alhodaib:** Software, Conceptualization. **Ammar Khan:** Resources, Conceptualization. **Mukhlisa Soliyeva:** Data Curation, Validation. **Vineet Tirth:** Writing – review & editing, Writing – original draft, Conceptualization. **Saima Naz Khan:** Writing – review & editing, Supervision. **Khizar Hayat:** Writing – review & editing, Supervision. **Amnah Mohammed Alsuhaibani:** Writing - review & editing, Visualization. **Moamen S. Refat:** Resources, Formal Analysis. **N.M.A. Hadia:** Conceptualization, Validation. **Asad Ali:** Writing – review & editing, Supervision. **Abid Zaman:** Writing – review & editing, Software.

Declaration of competing interest

The authors declare that they have no known competing financial interests or personal relationships that could have appeared to influence the work reported in this paper.

Data availability

Data will be made available on request.

Acknowledgment

This research was funded by the Universiti Kebangsaan Malaysia under Grant Code GGPM-2021-050 and GP-2021-K023619. The authors extend their appreciation to the Deanship of Scientific Research at King Khalid University Abha 61421, Asir, Kingdom of Saudi Arabia for funding this work through the Large Groups Project under the grant number RGP.2/545/44. Princess Nourah bint Abdulrahman University Researchers Supporting Project number (PNURSP2024R65), Princess Nourah bint Abdulrahman University, Riyadh, Saudi Arabia.

References

[1] Zyoud SH, et al. Linear/nonlinear optical characteristics of ZnO-doped PVA/PVP polymeric films for electronic and optical limiting applications. Crystals 2023;13(4):608.

[2] Saleem S, Jameel MH, Akhtar N, Nazir N, Ali A, Zaman A, et al. Modification in structural, optical, morphological, and electrical properties of zinc oxide (ZnO) nanoparticles (NPs) by metal (Ni, Co) dopants for electronic device applications. Arab J Chem 2022;15(1):103518.

[3] Kacem E, Althobaiti HA, Al-Ejji M, Bader N, Abed A, Rajeh A. Structural, optical, and thermal studies of Poly (vinylidene fluoride-co-hexafluoropropylene) and Polyvinylpyrrolidone doped Ag/ZnO mixed nanoparticles for flexible optoelectronic devices. Opt Mater 2023;146:114560.

[4] Al-Muntaser AA, Alzahrani E, Abo-Dief HM, Saeed A, Alshammari EM, Al-Harthi AM, et al. Tuning the structural, optical, electrical, and dielectric properties of PVA/PVP/CMC ternary polymer blend using ZnO nanoparticles for nanodielectric and optoelectronic devices. Opt Mater 2023;140:113901.

[5] Ahmed K, Mehboob N, Zaman A, Ali A, Mushtaq M, Ahmad D, et al. Enhanced the Cu^{2+} doping on the structural, optical and electrical properties of zinc oxide (ZnO) nanoparticles for electronic device applications. J Lumin 2022;250:119112.

[6] Sypniewskaa M, Szczesnyb R, Popielarskic P, Strzalkowskia K, Derkowska-Zielinskaa B. Structural, morphological and photoluminescent properties of annealed ZnO thin layers obtained by the rapid sol-gel spin-coating method. Opto-Electron Rev 2020;28:182–90.

[7] Yerişkin SA, Tanrıkulu EE, Ulusoy M. Dielectric properties of MS diodes with Ag: ZnO doped PVP interfacial layer depending on voltage and frequency. Mater Chem Phys 2023;303:127788.

[8] Alamgeer, Tahir M, Sarker MR, Ali S, Ibraheem, Hussian S, et al. Polyaniline/ZnO hybrid nanocomposite: Morphology, spectroscopy and optimization of ZnO concentration for photovoltaic applications. Polymers 2023;15(2):363.

[9] Mohammed MI. Controlling the optical properties and analyzing mechanical, dielectric characteristics of MgO doped (PVA–PVP) blend by altering the doping content for multifunctional microelectronic devices. Opt Mater 2022;133:112916.

[10] Rajesh K, Crasta V, Kumar NBR, Shetty G, Rekha PD. Structural, optical, mechanical and dielectric properties of titanium dioxide doped PVA/PVP nano. J Polym Res 2019;26(4):99.

[11] Sengwa RJ, Dhatarwal P. Nanofiller concentration-dependent appreciably tailorable and multifunctional properties of (PVP/PVA)/SnO_2 nanos for advanced flexible device technologies. J Mater Sci Mater Electron 2021;32:9661–74.

[12] Al-Hardan NH, Jalar A, Hamid MA, Keng LK, Shamsudin R, Majlis BY. The room-temperature sensing performance of ZnO nanorods for 2-methoxyethanol solvent. Sens Actuators B 2014;203:223–8.

[13] AlAbdulaal TH, Almoadi A, Yahia IS, Zahra HY, Alqahtani MS, Yousef ES, et al. High optical performance of Gd_2O_3-doped PVA/PVP films for electronic and laser CUT-OFF filters. Optik - Int J Light Electron Opt 2022;268:169741.

[14] Hashim A, Algidsawi AJK, Ahmed H, Hadi A, Habeeb MA. Structural, dielectric, and optical properties for (PVA/PVP/CuO) nanos for pressure sensors. НаносистеМи, наноМатеріали, Нанотехнології Nanosistemi, Nanomateriali, Nanotehnologii 2021;19(1):91–102.

[15] Choudhary S, Sengwa RJ. ZnO nanoparticles dispersed PVA–PVP blend matrix based high performance flexible nanodielectrics for multifunctional microelectronic devices. Curr Appl Phys 2018;18:1041–58.

[16] Sunaryono MF, Hidayat MN, Kholifah A, Aripriharta Taufiq N, Mufti M, Diantoro SS, et al. Study of nanostructural, electrical, and optical properties of

$Mn_{0.6}Fe_{2.4}O_4$–PEG/PVP/PVA ferrogels for optoelectronic applications. J Inorg Organomet Polym Mater 2020;30:4278–88.
[17] Sypniewska M, Szczesny R, Skowronski L, Kamedulski P, Gondek E, Apostoluk A, et al. Optical and morphological properties of ZnO and Alq3 incorporated polymeric thin layers fabricated by the dip-coating method. Appl Nanosci 2023;13(7):4903–12.
[18] Jędrzejewska-Szczerska M. ALD thin ZnO layer as an active medium in a fiber-optic Fabry-Perot interferometr. Sens Actuators A 2015;221:88–94.
[19] Abdolmaleki A, Mallakpour S, Borandeh S. Polym Bull 2012;69:15–28.
[20] Prakash Y, Mahadevaiah D, Somashekarappa H, Demappa T, Somashekar R. Microstructural parameters of HPMC/PVP polymer blends using wide angle X-Ray technique. J Res Updates Polym Sci 2012;1(1):24.
[21] Khan AD, Ikram M, Haider A, Ul-Hamid A, Nabgan W, Haider J. Polyvinylpyrrolidone and chitosan-doped lanthanum oxide nanostructures used as anti-bacterial agents and nano-catalyst. Appl Nanosci 2022;12(7):2227–39.
[22] Shahzadi A, Moeen S, Khan AD, Haider A, Haider J, Ul-Hamid A, et al. La-doped CeO_2 quantum dots: Novel dye degrader, antibacterial activity, and in silico molecular docking analysis. ACS Omega 2023;8(9):8605–16.
[23] Ikram M, Bari MA, Bilal M, Jamal F, Nabgan W, Haider J, et al. Innovations in the synthesis of graphene nanostructures for bio and gas sensors. Biomater Adv 2023;145:213234.
[24] Walbrück K, Kuellmer F, Witzleben S, Guenther K. Synthesis and characterization of PVP-stabilized palladium nanoparticles by XRD, SAXS, SP-ICP-MS, and SEM. J Nanomater 2019:1–7.
[25] Altındal Ş, Sevgili Ö, Azizian-Kalandaragh Y. The structural and electrical properties of the Au/n-Si (MS) diodes with nanos interlayer (Ag-doped ZnO/PVP) by using the simple ultrasound-assisted method. IEEE Trans Electron Devices 2019;66(7):3103–9.
[26] Gallardo-Sánchez MA, Chinchillas-Chinchillas MJ, Gaxiola A, Alvarado-Beltrán CG, Hurtado-Macías A, Orozco-Carmona VM, et al. The Use of recycled PET for the synthesis of new mechanically improved PVP nanofibers. Polymers 2022;14(14):2882.
[27] Chamakh M, Ayesh AI. Production and investigation of flexible nanofibers of sPEEK/PVP loaded with RuO_2 nanoparticles. Mater Des 2021;204:109678.
[28] Abdullah MM. Facile growth, physical characterization, and dielectric response of as-grown NiO nanostructures. J King Saud Univ-Sci 2020;32(1):1048–54.
[29] Jonscher AK. The'universal'dielectric response. I. IEEE Electric Insulat Magaz 1990;6(2):16–22.
[30] Dussan S, Kumar A, Scott JF, Katiyar RS. Effect of electrode resistance on dielectric and transport properties of multiferroic superlattice: A Impedance spectroscopy study. AIP Adv 2012;2(3).
[31] Funke K. Jump relaxation in solid electrolytes. Prog Solid State Chem 1993;22(2):111–95.
[32] Abdullah MM. Structural characterizations and frequency dependent dielectric properties of as-prepared $Gd2O_3$ nanorods. Curr Nanosci 2017;13(5):501–5.
[33] El Gohary HG, Qahtan TF, Alharbi HG, Asnag GM, Waly AL. Studies of the structural, optical, thermal, electrical and dielectric properties of a polyvinyl alcohol/sodium alginate blend doped with Cu nanoparticles and ZnO nanorods as hybrid nanofillers for use in energy storage devices. J Polym Environ 2023:P.1-11.
[34] Matysiak W, Tański T, Zaborowska M. Manufacturing process and characterization of electrospun PVP/ZnO NPs nanofibers. Bull Pol Acad Sci Techn Sci 2019;67(2):193–200.
[35] Ashiq MN, Iqbal MJ, Gul IH. Effect of Al–Cr doping on the structural, magnetic and dielectric properties of strontium hexaferrite nanomaterials. J Magn Magn Mater 2011;323(3–4):259–63.
[36] Zhang Q, Zhu X, Xu Y, Gao H, Xiao Y, Liang D, et al. Effect of La^{3+} substitution on the phase transitions, microstructure and electrical properties of $Bi1- xLa_xFeO_3$ ceramics. J Alloy Compd 2013;546:57–62.
[37] Ahmed I, Mustafa G, Subhani MU, Hussain G, Ismail AG, Anwar H. A detailed investigation of lanthanum substituted bismuth ferrite for enhanced structural, optical, dielectric, magnetic and ferroelectric properties. Results Phys 2022;38:105584.
[38] Yekkaluri SR, Konda S, Velpula D, Thida RK, Chidurala SC, Tumma BN, et al. Comparative analysis of ZnO nanoparticle's specific capacitance in supercapacitors: The role of surfactant and stabilizing agent. Appl Surf Sci Adv 2022;12:100326.
[39] Sun Y, Dang H, Huang N, Wang D, Liang C. Effects of surfactants on the preparation of MnO_2 and its capacitive performance. J Appl Biomater Funct Mater 2017;15(1_suppl):7–12.
[40] Saravanakumar B, Radhakrishnan C, Ramasamy M, Kaliaperumal R, Britten AJ, Mkandawire M. Surfactant determines the morphology, structure and energy storage features of CuO nanostructures. Results Phys 2019;13:102185.
[41] Alver ÜMİT, Tanrıverdi A, Akgül Ö. Hydrothermal preparation of ZnO electrodes synthesized from different precursors for electrochemical supercapacitors. Synth Met 2016;211:30–4.
[42] Reutov VE, Burkaltseva DD, Vorobieva EI, Blazhevich OG, Betskov AV, Kilyaskhanov KS, et al. Methodology for assessing the financial and economic security of the agro-industrial complex. Int J Recent Technol Eng 2019;8(2):4430–5.
[43] Shaheen I, Ahmad KS, Zequine C, Gupta RK, Thomas AG, Azad Malik M. Sustainable synthesis of organic framework-derived ZnO nanoparticles for fabrication of supercapacitor electrode. Environ Technol 2022;43(4):605–16.
[44] Rani N, Saini M, Yadav S, Gupta K, Saini K, Khanuja M. (2020, October). High performance super-capacitor based on rod shaped ZnO nanostructure electrode. In *AIP Conference Proceedings* (Vol. 2276, No. 1). AIP Publishing.
[45] Kumar R, Sahoo S, Joanni E, Singh RK, Kar KK. Microwave as a tool for synthesis of carbon-based electrodes for energy storage. ACS Appl Mater Interfaces 2021;14(18):20306–25.
[46] Gugulothu D, Barhoum A, Nerella R, Ajmer R, Bechelany M. Fabrication of nanofibers: electrospinning and non-electrospinning techniques. Handb Nanofibers 2019:45–77.
[47] Thenmozhi S, Dharmaraj N, Kadirvelu K, Kim HY. Electrospun nanofibers: New generation materials for advanced applications. Mater Sci Eng B 2017;217:36–48.
[48] Sadri M, Maleki A, Agend F, Hosseini H. Retracted: Fast and efficient electrospinning of chitosan-Poly (ethylene oxide) nanofibers as potential wound dressing agents for tissue engineering. J Appl Polym Sci 2012;126(6):2077.
[49] Ye XY, Liu ZM, Wang ZG, Huang XJ, Xu ZK. Preparation and characterization of magnetic nanofibrous composite membranes with catalytic activity. Mater Lett 2009;63(21):1810–3.
[50] Hassan MM, et al. Structural and frequency dependent dielectric properties of Fe^{3+} doped ZnO nanoparticles. Mater Res Bull 2012;47(12):3952–8.
[51] Li Z, Zhang H, Zheng W, Wang W, Huang H, Wang C, et al. J Am Chem Soc 2008;130:5036–7.
[52] Zamiri R, et al. Structural and dielectric properties of Al-doped ZnO nanostructures. Ceram Int 2014;40(4):6031–6.
[53] Pospisil P, Sýkora J, Takematsu K, Hof M, Gray HB, Vlček A. Light-induced nanosecond relaxation dynamics of rhenium-labeled Pseudomonas aeruginosa Azurins. J Phys Chem B 2020;124(5):788–97.